AirCargoChallenge 2022

# Technical Report

Team #16

AkaModell Stuttgart

AKAMODELL STUTTGART E.V.

## Table of contents

## List of Figures

Chapter 1

# Introduction

The Air Cargo Challenge is an important contest for AkaModell Stuttgart, in which it has participated four times, and won in 2009, 2013 and 2017. The new regulations [1] provide an opportunity to apply the knowledge acquired from previous projects: Apart from the Air Cargo Challenge, projects for different radio-controlled glider competition classes, each with specific requirements, have been successfully completed in the AkaModell Stuttgart. Air Cargo Challenge 2022 is a great chance to bring together the knowledge that has been gained in fields ranging from lightweight construction to efficient aerodynamics.

However, the 2022 ACC edition is also bringing a particular challenge because of the global Corona Crisis.

## 1.1 Akamodell Stuttgart

Akamodell Stuttgart is an association of students and academic staff at the University of Stuttgart. Our aim is to pursue the fascinating sport of R/C aeromodelling on an academic level. Since many of the members are graduating in aerospace engineering, it is more than just a hobby to them. It is a way to apply the rather theoretical knowledge from studies to the real world. Designing as well as building and flying a model aircraft is very rewarding and a great learning experience. To make flying even more fun, Akamodell members are travelling together to flying events and competitions several times a year. There are usually camps on airfields or even trips to the Alps to test the latest glider designs.

Akamodell Stuttgart e.V. was founded in 1978 and is the oldest club of its kind in Germany. With more than four decades of experience in designing and building model aeroplanes, the club can rely on a vast base of knowledge when new challenges emerge, like the Air Cargo Challenge. After a massive setback in 1999 when the old workshop burnt down, the members managed to re-establish the workshop at a new site. The new workshop is located on the university campus, right between the research institutes and it is equipped with all the machinery needed. In particular the 3D CNC milling machine enables us to build CAD designed aircrafts faster and with a higher degree of accuracy than before.

## 1.2 University of Stuttgart

Located in the state capital of Baden-Württemberg, the University of Stuttgart is situated in one of Europe's strongest economic regions. It is a research university with a strong focus on engineering and natural sciences. Approximately 24 000 students are enrolled here, about 1 700 of them graduating each year. The University of Stuttgart is a member of TU9, the association of the German Institutes of Technology. The university consists of ten faculties, one of which is the faculty for Aerospace Engineering and Geodesy. The 13 institutes of this department cover a broad range of research and educational topics. Their spectrum extends the "classical" aerospace focus to topics such as wind energy, satellite navigation or remote sensing.

## 1.3 Professor in Charge

Prof. Dr. Andreas Strohmayer, head of the Aircraft Design Department at University of Stuttgart's Institute of Aircraft Design, acts as Professor in Charge for the Team AkaModell Stuttgart.

In 2001 Professor Strohmayer graduated at TU München to Dr.-Ing. in the field of conceptual aircraft design. From 2002 to 2008 he was director of Grob Aerospace in Mindelheim, Germany, responsible for design, production, and support of the Grob fleet of all-composite aircraft as well as the development of a 4-seat aerobatic turboprop, a 7-seat turboprop and the SPn business jet. From 2009 to 2013 he was program director for a 19-seat commuter aircraft project in Metz, France, before setting up an EASA approved design organisation in Memmingen, Germany, holding the TC for a 6-seat turboprop to be produced in China. In 2015 he became professor for Aircraft Design in Stuttgart with a research focus on manned (hybrid-)electric flight ("Icaré 2" and "e-Genius") and scaled UAS flight testing.

## 1.4 Team Members

AkaModell Stuttgart's ACC 2022 team consists of Bachelor, and Master students. The team members are introduced in the following.

**Gregor Zwickl**

23, Team Leader and Pilot

Course of studies: aerospace engineering

Background: Gregor has flown aircraft since his early childhood and competes in In- and Outdoor aerobatics. He joined the Akamodell in 2019

**Lucas Kugler**

24, Course of studies: aerospace engineering

Background: Lucas has been flying model airplanes for 12 years and is flying F3F competitions actively since 2012. In this field, he won the Junior and the Team World Champion title at the 2014 F3F World championship in Slovakia and has also participated to the 2016 World championship in Denmark. He started his aerospace engineering studies at the University of Stuttgart in 2015 and joined the AkaModell at that time. He already participated at the ACC in 2017.

**Jannik Frank**

21, Course of studies: aerospace engineering

Background: Jannik has been flying model aircraft since 2012, with strong interest in flying, designing, and building thermal and slope sailplanes. He started his aerospace engineering studies in 2019 and joined the AkaModell in 2021.

**Yannick Schäfer**

21, Course of studies: aerospace engineering

Background: Yannick joined the Akamodell in 2020 to participate in the ACC. Since then he has taken leadership at the Akamodell as Vice-President.

**Tjalf Stadel**

21, Course of studies: aerospace engineering

Background: Tjalf joined the Akamodell in 2019 with no prior experience in building and flying model aircraft.

**Matthias Schmid**

29, Course of studies: mechanical engineering

Background: Matthias started flying aeroplane models when he joined the AkaModell in 2014. He was member of the ACC organisation team in 2015. The main topics of his studies are fluid dynamics and mechanical design.

Chapter 2

# Project Management

During the Air Cargo Challenge project there are many deadlines the team has to meet. Thus, proper time planning and resource management is one of the keys to success in the competition. Three pillars of project management are utilised as indicated in figure 1.


**Figure 2-1** Three pillars of project management.

## 2.1 Team meetings

Team meetings are held almost every week. These meetings were used to track how the project develops and to do the necessary planning. This includes discussions of the progress of individual tasks and coordination of the next steps to avoid double work and mistakes. In addition, a team meeting is an excellent place to exchange experience between team members.

## 2.2 Time management

During the last Air Cargo Challenges, the Akamodell learned a lot about time management. Especially during ACC 2009 when the team slipped behind the schedule, resulting in an extraordinary high workload the last six weeks before the competition. To avoid this, time management was assigned a high priority this time. The preparation of ACC 2021 started very early. At the beginning of 2021, because the competition was postponed to this year, the decision was made to change the design into a more complex one. Since then, the team tried to keep up with the schedule to be on Track for the Event.

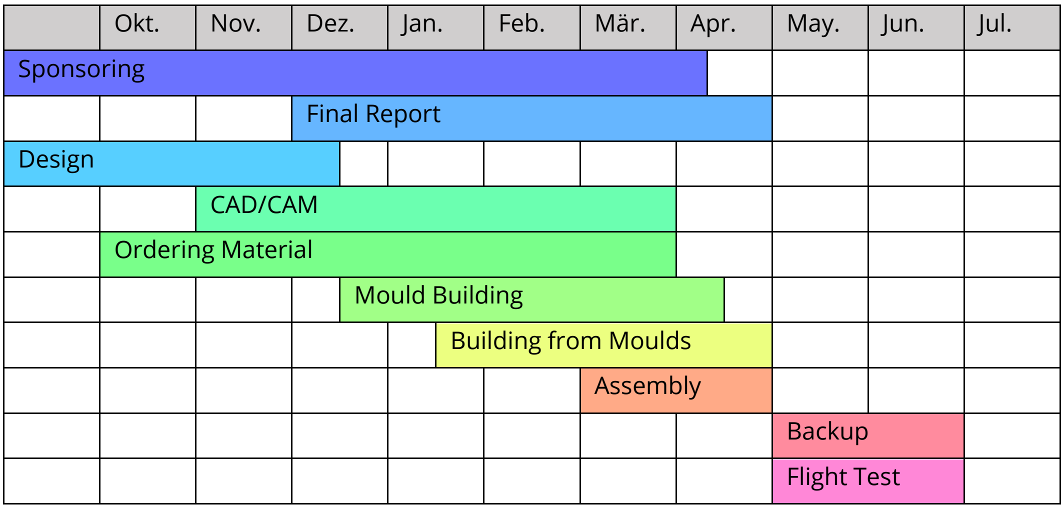

**Figure 2-2** Timeline for the preparation of the competition.

## 2.3 Human resources

The ACC project 2022 is very challenging for the team and results in many working hours. AkaModell's ACC 2022 team consists of students working on their studies and have their private life as well. For sure, every member of the team is unique in this context. To accommodate the differences, it was always tried to divide the work in different packages. For example, building the moulds is a lot of sanding work. A single person can finish a mould, and this work can be interrupted at any time without problems. On the other side, laminating the shells of the wing must be done by three people at the same time without interruptions. Only a good management of the different work packages and the personal situations of the team members will allow this project to succeed.

### 2.3.1 Sponsors

**MTU**

MTU Aero Engines AG is a German aircraft engine manufacturer. MTU develops, manufactures and provides service support for military and civil aircraft engines.

**CN Models**

CN-Models® unites people who like gliders and everything connected with them. Their products include the *Carboweave* carbon material, and the F3J/F5J models *Optimus* and *Sensor*

**Airbus**

Airbus SE is a European multinational aerospace corporation. Airbus designs, manufactures and sells civil and military aerospace products worldwide and manufactures aircraft in Europe and various countries outside Europe.

**METRO HOP**

Metro Hop promises to revolutionise the transport of passengers and cargo in urban environments.

**Vereinigung von Freunden der Universität Stuttgart**

**Verein der Freunde der Luft- und Raumfahrttechnik**

Chapter 3

# Aircraft Requirements

Most of the requirements the aircraft has to fulfil are listed in the regulations of the competition. Before designing an aircraft, it is important to know and understand all of the requirements. These can be separated into aircraft design and mission requirements.

## 3.1 Aircraft Design Requirements

The aircraft design requirements contain requirements which relate to the aircraft itself.

### 3.1.1 Configuration

Apart from the ban of rotary wings and lighter than air vehicles, the rules leave many options open for the configuration of the aircraft. This open design space in combination with the need for a high-lift configuration with a low span loading while reducing the penalty of operating at low Reynolds numbers has driven the choice of configuration to a conventional layout.

### 3.1.2 Propulsion

The motor and propeller are prescribed in the rules and the maximal tension of the battery is limited to 12.6V. This leaves only little room to optimise the propulsion components, except for the choice between two propeller manufacturers.

### 3.1.3 Structure

The structure needs to withstand both the flight loads and the structure validation test as specified in the rules.

The structural design and safety margins have to be balanced with the weight requirements for good performance, and techniques of lightweight design and construction need to be used.

### 3.1.4 Handling

This edition's flight task is less demanding than in the past, with no necessity to perform tight turns. However, sufficient manoeuvrability is still required, particularly in case of windy conditions. Furthermore, the first part of the climbing will be critical as it will likely be performed close to stall speed. Consequently, a good stall behaviour must be achieved, as a loss of control in this flight phase would have catastrophic consequences.

### 3.1.5 Manufacturing

The choice of materials and manufacturing techniques have been dictated by the required aerodynamic and structural performance on one hand, and the capabilities and experience of the AkaModell Stuttgart on the other. Since the club has a solid experience in designing and manufacturing fibre composite aircraft, a fibre composite structure built in milled negative moulds was chosen.

## 3.2 Mission requirements

The flight pattern prescribed by the rules has been divided into several mission segments to structure the analysis and optimization:

- Take-off
- Climb
- Cruise
- Landing approach and landing

The main requirement for the take-off is the 60 m maximal take-off distance, and the 40 m to benefit from the short take-off bonus. The climb is limited by the 100m limit to get full points, and the cruise depends on the altitude reached in the previous flight phase.

The segment for landing approach and landing has not been part of the mission optimization, although a close eye has been kept on handling and manoeuvrability to ensure a safe approach and landing.

Chapter 4

# Electronic systems & propulsion

To be able to fly the aircraft needs a propulsion and an electronic system to be steerable by the pilot. For the most part, the components of the powertrain are specified by the regulations, to provide an equal baseline for the competition between the teams.

The other electronic components, which are left open for the team to choose, are essential to be able to steer the aircraft. Due to their critical role for the controllability of the aircraft, of-the-shelf components are used here as well for their reliability.

## 4.1 Performance investigation

To learn important details on the propulsion system, such as the thrust at different airspeeds, wind tunnel measurements were conducted at the Institute of Aerodynamics and Gas Dynamics.

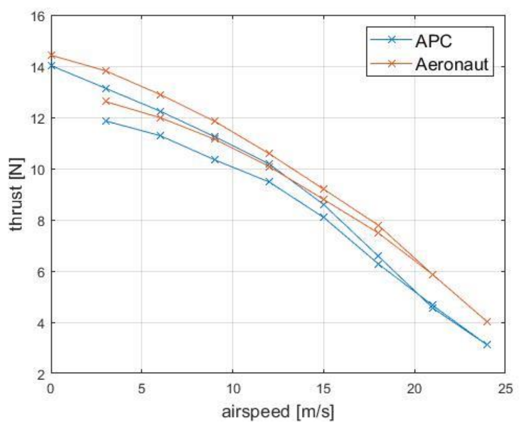


**Figure 4-1** Thrust over airspeed for the different propellers

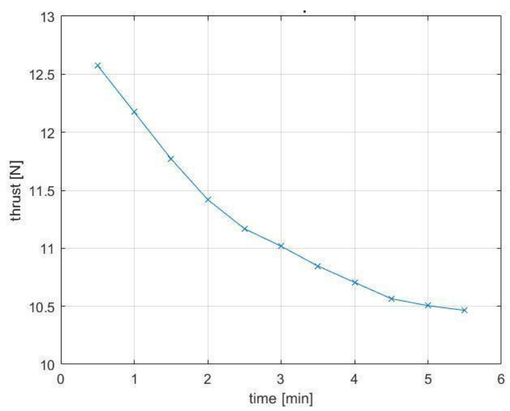


**Figure 4-2** Thrust over time at a constant airspeed of 9 m/s

Starting the test series, both the APC-E propeller and the Aeronaut propeller were measured in combination with the Kontronik Jive Pro 80+ controller. Then, the controller was changed to the Kontronik KOBY 55 LV to remeasure the Aeronaut propeller for comparison.

Each test series for the propellers started at 0 m/s airspeed. Then the thrust was measured at full throttle for a few seconds, after which the airspeed was increased by 3 m/s. The cycle continues up to 24 m/s and back again to 3 m/s. This revealed the hysteresis of the thrust as a result from decreasing battery power. Also, this would help identify measurement errors.

The final test was a continuous power run of 5 minutes at the constant airspeed of 9 m/s with the Aeronaut propeller, showing the decrease of thrust over time. Additionally, the battery voltage was monitored to ensure sufficient power during the flight. Therefore, the Jive Pro controller was installed and connected to a UniLog2 data logger, since this was not possible with the KOBY 55. The logger was connected to a computer via USB, where the live data could be seen.

The data shows that the Aeronaut propeller generates an average of 11.6% more thrust than the APC propeller.

Insignificant however, is the difference comparing the two controllers (0.5% difference), thus leading to a decision by weight of the components.

Furthermore, it was established that the power of a 3000 mAh battery is sufficient to supply power during flight. These results are the basis for further development and therefore of great importance to the design process.

**Figure 4-3** The test stand mounted in the wind tunnel

## 4.2 Components

The former described design requires powerful and reliable components. Especially Servos must perform well in all flight conditions. The selected components are presented in the following sections.

### 4.2.1 Servos

For the sake of rationalisation, it was decided to use the same servos on all surfaces. Having a 4-part wing means that the flaps and ailerons are comparatively small. This gives the opportunity to use the same small servos in the wing as on the tail. Due to its excellent performance for the size, good reputation of the brand and availability, the MKS-HV6120H was selected to be used on all surfaces. This is an 8mm servo with a weight of 11g. It has a maximum torque of 5.4kg/cm.

### 4.2.2 Controller

In the past the Akamodell made good experiences with Kontronik ESCs and still has two different ones from the previous ACC competitions in the workshop. While doing our propeller measurements both models were compared, and no significant performance differences could be found. Therefore, it was decided to use the lighter one. This is the Kontronik *KOBY 55 LV*.

### 4.2.3 Radio

The choice of the radio system is up to the pilot. It is important that he feels comfortable with it as well as being reliable. Thus, we will probably use the Graupner Hott system. This system provides a sufficient reach and reliability for the flight task at hand. A minimum of 10 channels is needed for the receiver, therefore the GR-24 receiver was selected.

### 4.2.4 R/C Battery

Due to safety reasons, a separate battery pack will be used to supply power to the receiver and the servos. A 2S lipo battery was selected. Out of previous experience, it is expected that the minimum prescribed capacity of 600 mAh will be used, as it will be sufficient for the short flights of only 4-5 min.

Chapter 5

# Aircraft conceptual Design

To get the best overall design the requirements of different aspects had to be balanced.

## 5.1 General Configuration and Lessons Learned

In 2007, 2009, 2013 and 2017 AkaModell competed at the Air Cargo Challenge very successfully. The basic configuration of our planes, as it is pictured in figure 4, turned out to be effective and reliable. More experimental configurations were less convincing at past competitions. This year's rules lead us to depart from the "thin fuselage with cargo bay approach. Indeed, the low density of the water

**Figure 5-1** Evolution of airplane geometries from 2007 to 2017 (clockwise: ACC Akut, Heavy Heron, Goliath Heron and Zigzag Heron).

payloads makes for a noticeably higher cargo volume compared to previous editions, even though the payload weight is lower. After careful consideration we decided the best configuration was a large fuselage holding the cargo, with a high wing. The fuselage has a lid on top to allow for loading of the cargo. The high wing allows for enough ground clearance for the wing during take-off and landing.

In the following subsections the approach towards an effective aircraft design is described.

## 5.2 Mission Specific Optimisation

As pointed out in section 3.2, the aircraft has to handle three main tasks during a flight: take-off, climb and cruise. The flight path consists of following sections with specific demands:

- Rolling on the ground: minimum rolling friction and aerodynamic drag in ground effect
- Lift-off: maximum lift
- Acceleration and climb: quick acceleration to maximum climb speed
- Cruise: minimum drag
- Landing: structural robustness

All of them affect the score, hence a one-point optimisation is not suitable. To take into account the whole flight path from rolling on the ground to the final crossing of the line, a spreadsheet-based time-domain simulation has been developed. A schematic representation of this simulation is shown in **Figure 5-2**.

From given aerodynamic coefficients, given take-off mass m (empty weight estimated according to section 5.6 plus payload), rolling friction coefficient and measured thrust values the required take-off rolling distance can be determined. This has been done using a spreadsheet by explicit time integration and a look up table for drag $D$ and thrust $T$ values at the velocity $v$ corresponding to each time step $n$ (5-1). Acceleration a as well as velocity $v$ is assumed to be constant during each increment $\Delta t$ (5-2). The distance $s$ covered is accumulated (5-3).

$$v_n = v_{n-1} + a(v_{n-1}) \cdot \Delta t \qquad \text{5-1}$$

$$a(v) = \frac{T(v) - D(v)}{m} \qquad \text{5-2}$$

$$s_n = s_{n-1} + v_{n-1} \cdot \Delta t \qquad \text{5-3}$$

By means of this simulation, the impact of all relevant parameters on the score can be investigated. The goal has been to find an optimum design. However, some constraints that cannot be expressed in a mathematical way, like air and ground handling of the plane, pushes the design away from the theoretical optimum. The simulation was used to generate a first impression about the sensitivity of the flight score on several parameters. It turned out the maximum lift at Take-off (which is dominated by the wing area and the maximum lift coefficient) has the biggest influence. It also became clear the 10% Bonus for short take off should be aimed for, as it is generally larger than the points lost due to the lower payload.

Furthermore, an impression of the range of lift coefficient and Reynolds number during take-off, cruise and turns was gained. This information was used for airfoil

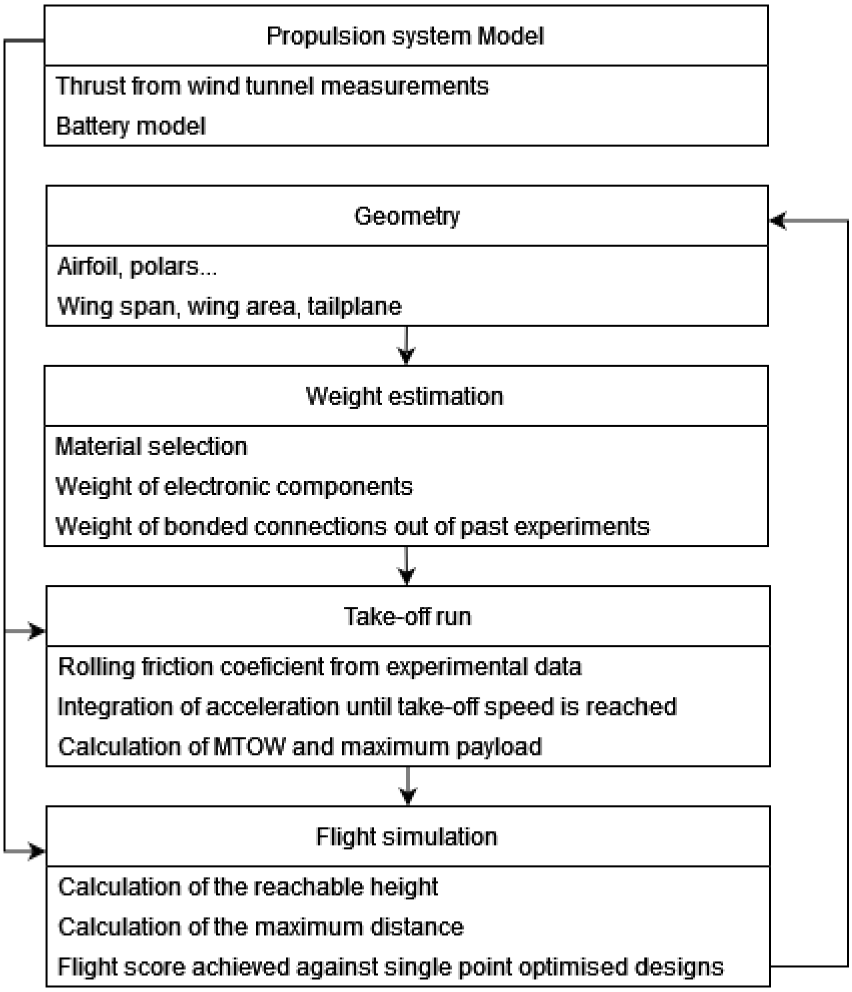


**Figure 5-2** Schematic representation of the simulation loop

design (section 0). The tail lever also proved to be one of the main limiting factors, and some wingspan had to be sacrificed to allow for a longer tail.

To solve the contradicting requirements of good take-off and in-flight performance, and taking inspiration from real world aircrafts, it was decided to implement a high-lift system comprised of fowler flaps. Such a system promises high-lift performance far outside the range of conventional single-element airfoils, while maintaining the latter's low drag in the clean configuration. This design decision however brought numerous challenges, in terms of construction, kinematics and aerodynamics.

## 5.3 Payload Integration

Due to its high volume, the payload is stored within the fuselage.  The bags are stored in an upright position and loaded from the top. the stiffening frames help to avaid any unwanted movement of the bags in flight. If a section of the payload bay is not full, XPS blocks can be used as spacers.

## 5.4 Fuselage, Landing Gear and Propulsion System Integration

Two different configurations of fuselage and cargo-bay were considered: a) separated fuselage and payload bay (as used in previous Akamodell designs), and b) an integral solution with the cargo in the fuselage.

It was found that both options where aerodynamically comparable: the first option had a higher wetted area but allowed to keep a higher fraction of the cargo-bay out of the propeller slipstream. However, the number of molds to be manufactured was higher and consequently the integral design was selected.

The fuselage is connected to the wing via 2 pins on each side which transfer the loads into the fuselage structure (the joiner does not transmit any loads to the fuselage). In these positions the shell is reinforced with a carbon plate instead of Rohacell sandwich material, and the structure is furthermore reinforced by 2 frames located at the same position. A tricycle landing gear is used for two reasons: it provides good directional stability during the take-off run and allows time-accurate rotation for lift-off. The main landing gear is a commercial off-the-shelf part, and the front landing gear strut is made from a Carbon Tube. The area where the fuselage is connected to the landing gear is also reinforced with a carbon fibre plate, and an additional half-frame. The Frame connecting both the rear wing-pins and the landing gear is especially reinforced, as it carries a significant part of the loads during landing.

## 5.5 Structural Design

The bending load of an aircraft wing is almost carried solely by the wing spar. For calculation purposes it is sufficient to take only the wing spar into consideration. The wing’s root bending moment resulting from lift can be calculated by integrating the lift distribution along the wingspan.

Two load cases are considered. For the first case, maximum lift during a turn with the highest occurring speed according to the simulation described in section 5.2 was used. The second case is the structural validation test at the competition, when the plane must withstand the load from being supported at the wing tips being fully loaded. A concentrated load of 70 N, corresponding to the maximum take-off mass, acting at the centre of the wing is assumed for this load case.

A safety factor of 3 is applied to dimension all components to account for gust loads and manufacturing imperfections.

Integration of the lift along the wingspan b using equation (5-4) results in the normal force $F_N(y)$ on the wing spar shear web for the flight case. For the structural validation test case, each half wing must bear a constant normal force of half the concentrated load. Integration of the normal force along the wingspan using equation (5-5) results in the spar bending moment. For an exact calculation the weight of the wing itself has to be considered before integration. This is not necessary in this case because the weight of the wing is negligible compared to the total weight.

$$F_N(y) = \int_{y=-\frac{b}{2}}^{0} n \cdot c_{l,max}(y) \cdot \frac{\rho}{2} v^2 \cdot c(y) dy \qquad 5\text{-}4$$

$$M_b(y) = \int_{y=-\frac{b}{2}}^{0} F_n(y) dy \qquad 5\text{-}5$$

For structural dimensioning, the maximum values of both load cases at the corresponding spanwise position are relevant. With the known bending moment along the wingspan the wing spar stress σ can be calculated according to equation (5-6).

$$\sigma_{max}(y) = M_b(y)\frac{z_{max}(y)}{I_x(y)} \qquad 5\text{-}6$$

Therefore, the moment of inertia of area $I_x(y)$ must be determined. The moment of inertia depends on vertical distance, width, and cross section of the spar flanges. The maximum distance of the spar flanges to the neutral axis is described by $z_{max}$. By rearranging the equation and inserting the maximum allowable stress of the used carbon fibres, the necessary cross section area can be calculated.

The wing torsional stiffness should be as high as possible. Otherwise, a torsional wing deformation could occur during flight and decrease the outer wing sections angle of attack and thereby its lift. Additionally, wing flutter could become an issue.

The aim is to build a wing as stiff as possible at a very low weight. To achieve this, we use high modulus carbon spread tow fabric. For estimation of the resulting stiffness and to provide a comparison of different carbon fibre lay-ups the D-box can be simplified as a closed shell. For closed, thin shells the polar moment of inertia can be calculated with the Bredt-Batho equation 5-7.

$$I_T = \frac{(2 \cdot A_M)^2 \cdot t}{U} \qquad 5\text{-}7$$

$A_m$is the enclosed area of the shell; $t$ is the thickness of the shell and $U$ the circumference. The torsional stiffness $k_t$ of the wing can now be calculated with equation (5-8), where $G$ is the shear modulus and $b$ the wingspan.

$$k_t = \frac{G \cdot I_t}{b/_2} \qquad 5\text{-}8$$

It is obvious that the wing's torsional stiffness for a given cross section size depends solely on the shear modulus and the thickness of the shell. A thicker shell means more carbon fibre layers and thus more weight. Accordingly, we increased the shear modulus by using high modulus spread tow tissue. The mechanical properties of the different fibre types used are compiled in Table 5-1.

It should also be mentioned that the shear modulus of the carbon layer cannot easily be extracted from material tables because the carbon layer is used in a 45° orientation. Therefore, for an exact calculation classical laminate theory (CLT) must be applied. Furthermore, the pure fibre properties cannot be transferred to a laminate, especially under compression load. Therefore, own experimental data obtained during the preparation for ACC 2007 was used.

In lightweight structures, it is often seen that skin buckling is more critical than torsional strength of a wing. The buckling resistance of the wing was estimated according to [7]. Ribs were considered, but the analysis of buckling resistance showed that they were not necessary.

## 5.6 Weight estimation

To find the optimum aircraft geometry a reliable mass calculation is necessary. For this, the sizing spreadsheet contains a mass estimation module. Based on the geometry of the aircraft, and the layup and materials that are to be used, the weight of the shells and spars are calculated. The data from past experiments is used to estimate the weight of resin used to bond the elements together. This tool has been improved over time, using the actual weights of the finished airplanes to refine the calculations. It does not however calculate the weight of the kinematics, as they have never been built before. Therefore, the weight of these elements was estimated based on data from the CAD model. A breakdown of the main components can be found in Table 5-2.

**Table 5-1** Fibre properties [9]

| Fibre | E-glass | High tensile carbon (HTA40) | High modulus carbon (UMS40) |
|---|---|---|---|
| Tensile strength [MPa] | 3400 | 3950 | 4560 |
| Young's Modulus [GPa] | 73 | 238 | 395 |
| Elongation at break | 3.5-4 % | 1.70% | 1,10% |
| Used fabrics | Roving,<br>plain weave: 49g/m²,<br>twill weave: 163 g/m² | Roving,<br>plain weave: 80 - 160 g/m²<br>non-woven biaxial: 150g/m² | Non-woven biaxial: 20, 30 and 40 g/m²<br>uni-directional: 100 g/m² |

**Table 5-2** Breakdown of the weight estimation

| Component | Weight [g] |
|---|---|
| Wings | 700 |
| Kinematics | 100 |
| Fuselage | 100 |
| Landing gear | 40 |
| Motor | 181 |
| Propulsion Battery | 269 |
| Receiver battery | 40 |
| Controller | 55 |
| Servos | 88 |
| Tailplane | 50 |
| Cables | 30 |
| Margin | 100 |
| **Sum** | **1753** |

## 5.7 Payload prediction

The payload in dependence of air density ρ was predicted by means of the simulation described in section 5.2. A linear interpolation is specified by equation 5-9. In Figure 5-3, a graphic representation of the equation is shown.

$$Payload\ [kg] = 2.5[m^3] \cdot \rho \left[\frac{kg}{m^3}\right] + 0.925[kg] \qquad \text{5-9}$$

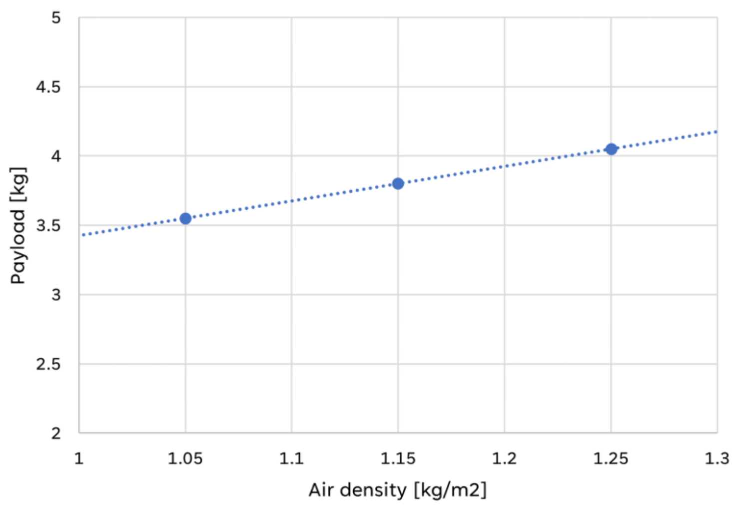


**Figure 5-3** Estimated payload over air density

Chapter 6

# Aerodynamic design

To achieve the best aerodynamic performance, a new airfoil has been designed and tested afterwards in the wind tunnel. With this information the wing geometry was developed.

## 6.1 Airfoil design

The design of the airfoil is driven by the requirements that are linked to each of the 3 flight phases:

- High maximum lift at take-off, to allow for a high payload, at Re 150 000
- Low drag during the distance flight, at Re 400 000
- Good lift-to-drag ratio during climb

The challenge with these requirements being that the first and second requirements strongly contradict each other. The airfoil efficiency during climb is of lesser importance, as the climbing performance is dominated by the available thrust and the induced drag.

The first approach was to try to balance these contradicting requirements as well as possible in a conventional airfoil. A first Airfoil was obtained by using the optimisation algorithm XOptFoil linked to Xfoil [2]. This design showed promising performance but was quite radical. It was therefore questionable if the predicted performance would be met in a real application.  In parallel another airfoil was designed manually with Pr. Eppler's software *Profile*. This design was more conservative, but the predicted performance was lower. A comparison of both airfoils can be seen in Figure 6-1. Both airfoils rely on heavy rear loading of the airfoil to generate high lift, while having a very low-pressure recovery on the upper side to delay stall.

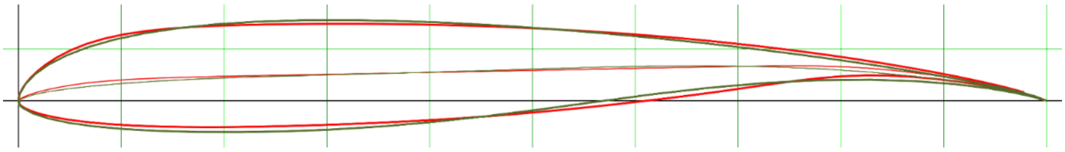

**Figure 6-1** The first airfoil designs, *XOptFoil* result in red, manual design in *Profile* in green.

It seemed necessary to test both sections in a wind tunnel to know which of them had the best real-world performance. However, at the time these plans arose, the postponing of the competition was announced, and it was decided to make use of Fowler flaps. This led to a new start with the airfoil design.

Very few two element sections designed for low Reynolds numbers are publicly available, and literature is sparse on the subject, as the smallest use cases are general aviation aircraft [3] [4]. A custom airfoil would therefore need to be designed. To reduce the complexity of the task at hand, it was decided to reuse the acc17 Airfoil for the clean section, as it has been used in the past and showed great performance. The problem therefore was narrowed down to the design of the flap leading edge, and the positioning of the extended flap, while considering the kinematic constraints.

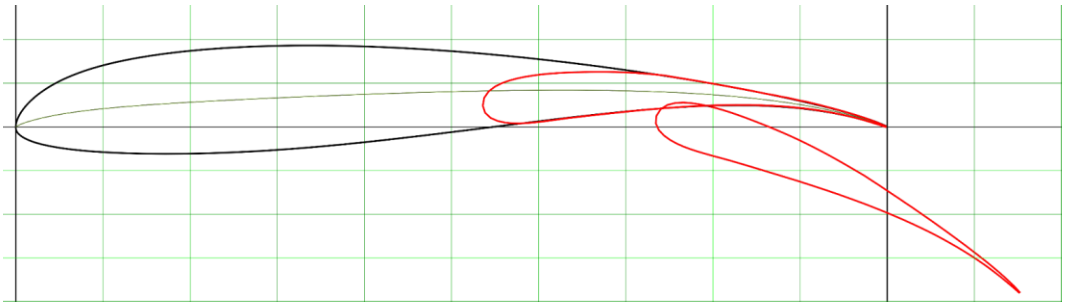

**Figure 6-2** The final fowler flap design, *acc22_v19*. Flap depicted in extended and retracted position

The resulting design, shown in Figure 6-2, named acc22_v19 has a flap with a depth of 47%; in extended position, the cord is increased by 18%. The performance of the fowler flap at take-off is unmatched. The additional weight due to the actualtion mechanism must however be considered.

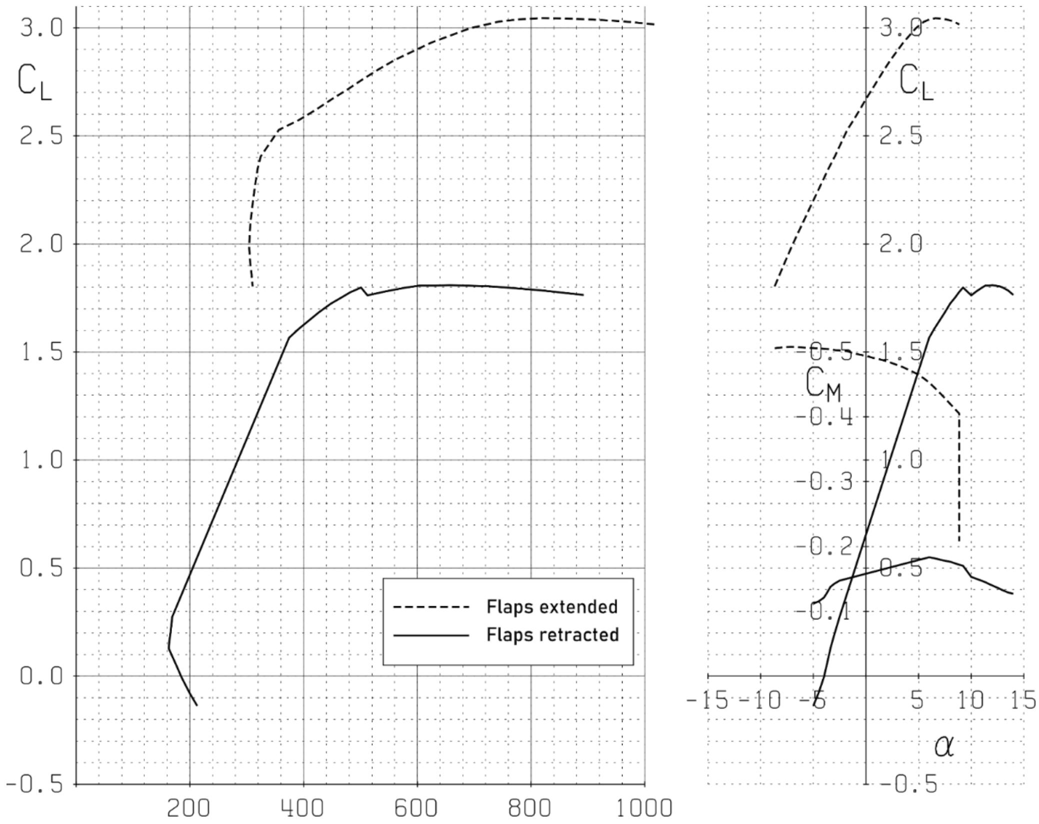


**Figure 6-3** Simulated Polar of the airfoil *acc22_v19*, at 150 000 Reynolds

During the design of the airfoil, it was noticeable that the leading-edge shape, and the position of the flap in its extended position had a significant effect on the maximum lift. As little was known about the accuracy of the simulations at very low Reynolds numbers (150k at take-off) it was again decided to perform wind-tunnel measurements of the airfoil, which would furthermore allow to optimise the flap positioning.

## 6.2 Wind tunnel testing

Following the calculations, wind tunnel measurements were conducted in November 2021 in the model-wind-tunnel at the Institute of Aerodynamics and Gas Dynamics. A Model was therefore built out of GFRP. The flap itself was fitted to the main wing on an aluminium support structure, also indicating the position, which allowed easy manipulations of the deflection angle and slot-size, as can be seen in Figure 2-1. The size was determined to allow Reynolds numbers of 150 000.

In the measuring series, all possible combinations of slot-size (in height and length) and deflection angle were tested around the ideal position determined by the calculations. For each combination, the range of angles of attack relevant to the maximum lift were measured. For the most interesting combinations, complete polars including the hysteresis were measured.

The results from the test series have validated the calculations with MSES. Furthermore, an even greater maximum of cl was achieved compared to the calculation, as depicted in Figure 6-5. However, the results near the maximum lift coefficient are to be interpreted with caution. It is likely, that the true figures are lower because the blockage ratio of around 10% at high angles of attack with the extended flap has an acceleration effect on the airflow, increasing the lift. This is typically corrected by the wind-tunnels software, however the lift coefficients measured fall outside the range of validity of these formulas. Calculations with fixed domain boundaries were also performed to mimic the effect of the wind tunnel; they indeed show an increase of lift compared to free flow conditions, but this increase is too small to explain the very $c_{l,max}$ that was measured.

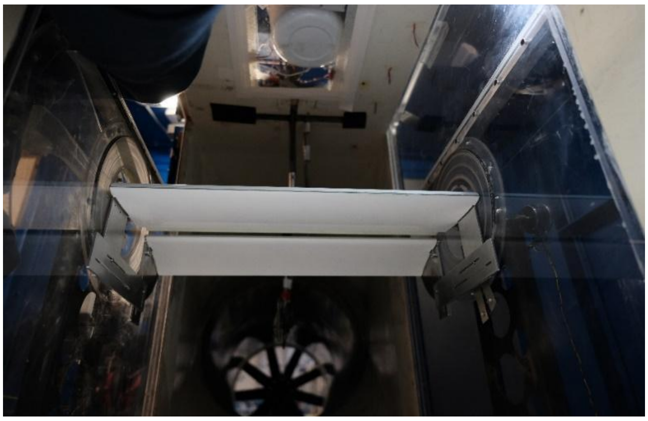

**Figure 6-4** The model installed in the wind tunnel.

Nevertheless, these results are a promising proof of concept, showing that the design does have a great effect on the lift coefficient, and therefore the take-off performance.

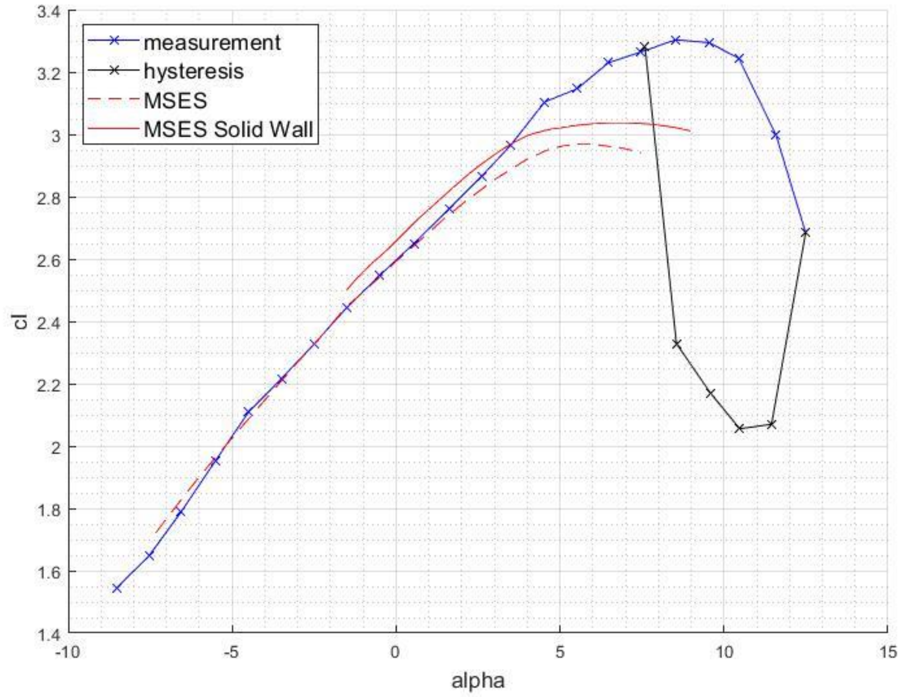


**Figure 6-5** Lift polar (lift ceficient over angle of attack) compared to simulated polar for the extended flap.

## 6.3 Wing Geometry

Contrary to previous editions, the wing geometry design was not only dictated by aerodynamic concerns.

The requirement to fit the aircraft in a Rhombus led to the use of a swept back outer segment, so to allow the wing to be shifted forward. The basic wing geometry was designed as close as possible to an elliptical plan form while keeping a sufficient tip chord, as sufficient space was needed to house the flap actuation mechanism.

Another challenge lay in the design of the ailerons. The original concept was to use the entire flaps as ailerons. This however led to many constraints on the airfoil design to allow the flap to be moved in the retracted position. The second option that was studied was to have a fowler flap only in the inner section of the wing, with conventional flaps outside. The reduced complexity came at the expense of performance, however, with questions being raised about the increase of induced drag due to the interruption of the flaps. Ultimately the solution was found by integrating a movable aileron within the outer flap.

A dihedral of 1° half angle at the centre and 5° at the tip panels was chosen from experience to ensure spiral stability and sufficient rudder effectiveness.

The different solutions were modelled in OpenVSP to perform a VLM analysis and compare the induced drag and lift distribution of the wing .

## 6.4 Empennage and Stability

A T-tail was chosen because it provides more downforce than other configurations for rotating the plane during take-off, since the elevator is outside the downwash of the wing. Additionally, trim drag during cruise is reduced. The tail volumes are determined by static stability and based on values from previous aircraft and literature values [6]. Because of the varying wing chord when the flaps are deployed, the aircraft has an unusually high static margin in the take-off phase, and the horizontal tailplane must be oversized accordingly. All lateral and longitudinal dynamic modes are sufficiently damped due to the concentration of mass near the centre of gravity. Based on experience, the longitudinal static margin $ST$ according to equation 6-1 was chosen to 10% of the mean aerodynamic chord $c_{MAC}$. $X_n$ denotes the neutral point $x$ coordinate and $X_{CG}$ the $x$ coordinate of the centre of gravity. The centre of gravity position will be finally adjusted during flight testing. The empennage will be manufactured from balsa wood and covered with film due to ease of manufacture and low weight.

$$ST = \frac{X_n - X_{CG}}{c_{MAC}} \qquad 6\text{-}1$$

The tail volume coefficients, lever arms *r* and areas *S* are summarised in the following table.

**Table 6-1** Tailplane dimensions

| | Volume Coefficient | R [m] | S [m²] |
|---|---|---|---|
| Horizontal Tail | 0.583 | 0.65 | 0.141 |
| Vertical Tail | 0.018 | 0.67 | 0.045 |

Chapter 7

# Manufacturing Techniques

The manufacturing methods used were mostly proven and tested in previous projects, but new techniques also had to be developped. All major parts are manufactured in negative molds with composite material. In the following subsections the manufacturing process is described in detail.

## 7.1 Wing

The wing consists of an upper and a lower fibre composite sandwich shell. The shell is composed of an outer layer of carbon fibre, followed by a foam support material. The inner layer is once again carbon fibre, with weights ranging from 20 to 40 g/m², depending on the location within the wings. Critical areas were further supported by carbon fibre fabrics. The wing is divided into four sections, each of which having an upper and lower mold. Additionally, there are four corresponding sections for the flap. The molds are milled from polyurethane material with our CNC milling machine. Because of the porous surface quality, it was necessary to coat the molds with a polyester spray filler. The coat was then sanded down to an even surface before applying a release agent and a layer of paint. Then, the sandwich structure was laminated into the molds and vacuum cured.

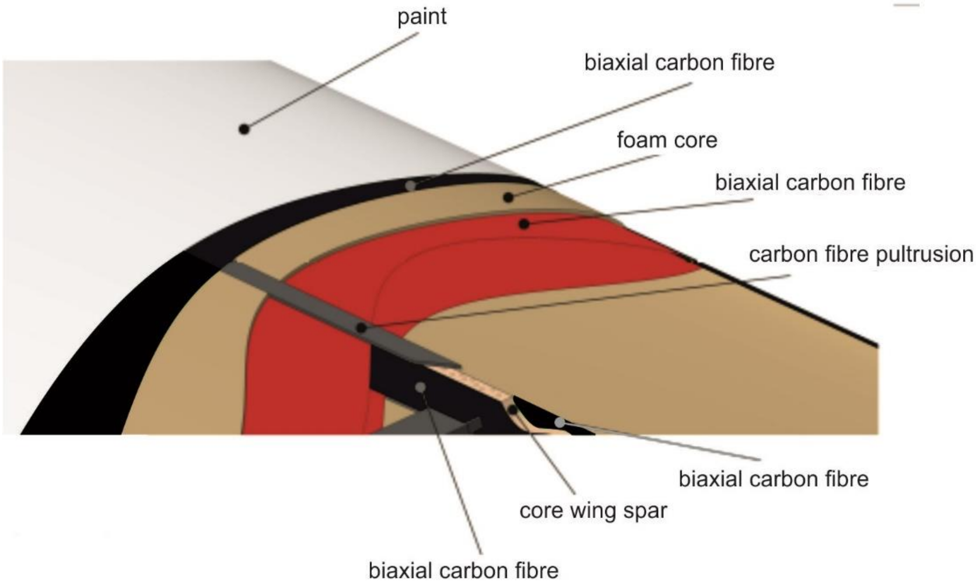


**Figure 7-1** Exemplary layup of the wings

**Figure 7-2** The milling machine during the production of one of the molds

The most critical part of the wing manufacturing is the inner structure. It is critical for joining the wing sections, prevention of buckling and, most importantly, operating the flap. Both edges of the sections are supported with ribs milled from carbon fiber sandwich material. The spars are a combination of carbon flat sections and a carbon-balsa sandwich material, which we produced ourselves. The structure also includes glass-fiber sockets for the wing joiners, holding a small innovation. For the first time we managed to use vacuum-curing on the sockets, which are built directly on the corresponding wing joiners, without applying too much pressure to not be able to release them from the sockets. This resulted in a significant increase in surface quality and a reduction of weight by several grams. The internal flap mechanism is produced in the CNC mill from carbon fiber plates and sever metal components.

**Figure 7-3** The resin printed molds for the center rail

The most innovative and challenging parts were the flap track rails. Each wing has three different rails, a both-sided rail in
between the flaps and one on each end. The complex geometry makes them unsuitable for conventional manufacturing techniques. The wingtip rail is the smallest rail with, which allowed it to be milled from aluminum in a 5-axis CNC mill at the Institute for Machine Tools.

The center rail is the most complex part, which is challenging to manufacture, even with a 5-axis CNC mill. Therefore, a first approach was taken with 3D-printed rails using PETG. This resulted in two problems. The surfaces on one side are of poor quality because of the support structure necessary for the printing process. Additionally, while the tensile strength would be sufficient, the deformations are too high due to the low stiffness of the material.

The second approach was then to experiment with molds from a Formlabs 2 resin printer. The complex geometry led to molds composed of 3 to 5 sections which are coated with a PVA release agent. The tracks are then laminated using short carbon fibre resin and rovings. This led to exceptional mechanical strength combined with outstanding surface quality.

**Figure 7-4** The centre rail directly after demolding

## 7.2 Fuselage and Landing Gear

Unlike the previous ACC designs of the Akamodell Stuttgart, the volume of the payload lead to the decision to have the payload stored in the Fuselage, without an external payload bay. This means that the cross sections and surfaces are much higher than on the previous very thin fuselages. In the past the Fuselages have been built out of monolithic carbon fibre, using a pressure bladder for molding.

With the new fuselage design, this method was not suited anymore, as it would have led to excessive weight, unnecessary strength, and manufacturing problems due to the high forces on the molds with the pressure bladder process. Therefore, it was decided to build the fuselage in a carbon-Rohacell sandwich construction similar to the wing shells. This sandwich is reinforced at strategic positions (Wing connections, landing gear fixations) with carbon plates placed in cut-outs in the sandwich material. Furthermore, the fuselage is reinforced with frames. Their Role is to stiffen the fuselage shells, carry the loads (particularly the load path between wing and landing gear mounting positions) and help maintain the payload bags in position.

Due to the size of restrictions on the transport box, the fuselage had to be designed in two parts, connected with a conical mating interface

Chapter 8

# Flight testing

Considering the aircraft was still under construction at the time of writing the report, this section will mainly deal about the planned methodology.

The first flights will mostly serve for the pilot to get accustomed to the aircraft's behaviour and to roughly set the travel of the control surfaces. They will be flown with reduced payload, and with only one flap position.

Once the basic settings have been sorted out, we will start the first flap transitions. It is likely that an intermediate flap position will be necessary to accelerate to a sufficient speed for the clean airfoil to sustain flight without stall. Indeed, as can be seen in Figure 6-3 the polars barely intersect.

The maximum payload will then be determined, as well as the optimum centre of gravity of the aircraft, as the latter plays an important role in the aircraft handling characteristics.

Once these initial tests have been done, additional flights will be made to find the best flight strategy for the competition. This means to determine the best climbing speed, for the pilot to get accustomed to fly as close as possible to the optimum point of the flight envelope.

The climb will be performed with retracted flaps, as the induced drag and trim drag are high when the flaps are extended. However, it will probably be necessary to first reach a safe altitude for the flap retraction.

Chapter 9

# Conclusion and Outlook

There are now only a little bit more than two months left until the begin of the competition.

Having one additional year of preparation time the Akamodell decided to go for a more complex project than the previous ones, because our competitors had this extra time too. For sure the goal is to defend the victory.

Combined with the fact that our team members couldn’t meet for a long time because of Covid-19, the complexity of our actual aircraft led to various delays.

Therefore, there is still a lot of work to do. In the upcoming two months the installation of the kinematic in the wing parts must be finished and the wings have to be closed. Also, the fuselage isn’t built yet.

Although the competition hasn’t started the Akamodell and its team members have already taken a lot of valuable knowledge from the participation. We are looking forward meeting the other Teams and Organisers and having a great competition in Munich!

## References

1: Air Cargo Challenge 2022 organizing committee : Requirements, Rules and Evaluation for the Air Cargo Challenge 2022. Munich, 2021.

3: Drela, M.: XFOIL: An Analysis and Design System for Low Reynolds Number Airfoils. Springer Berlin Heidelberg, 1989.

2: Florjancic, D.: Improved Design of a High Lift System for General Aviation Aircraft. Delft University of Technology, 2015

4: Wentz, W.: Development of a Fowler flap system for a high-performance general aviation airfoil, NASA, 1974.

6: MIT Lab Notes : Basic Aircraft Design Rules. Drela, M., 2006.

7: Wiedemann, J.: Leichtbau Elemente und Konstruktion. Springer-Verlag Berlin Heidelberg, 2007.

9: Toho Tenax Europe GmbH : Fibre portfolio and properties, 2008.

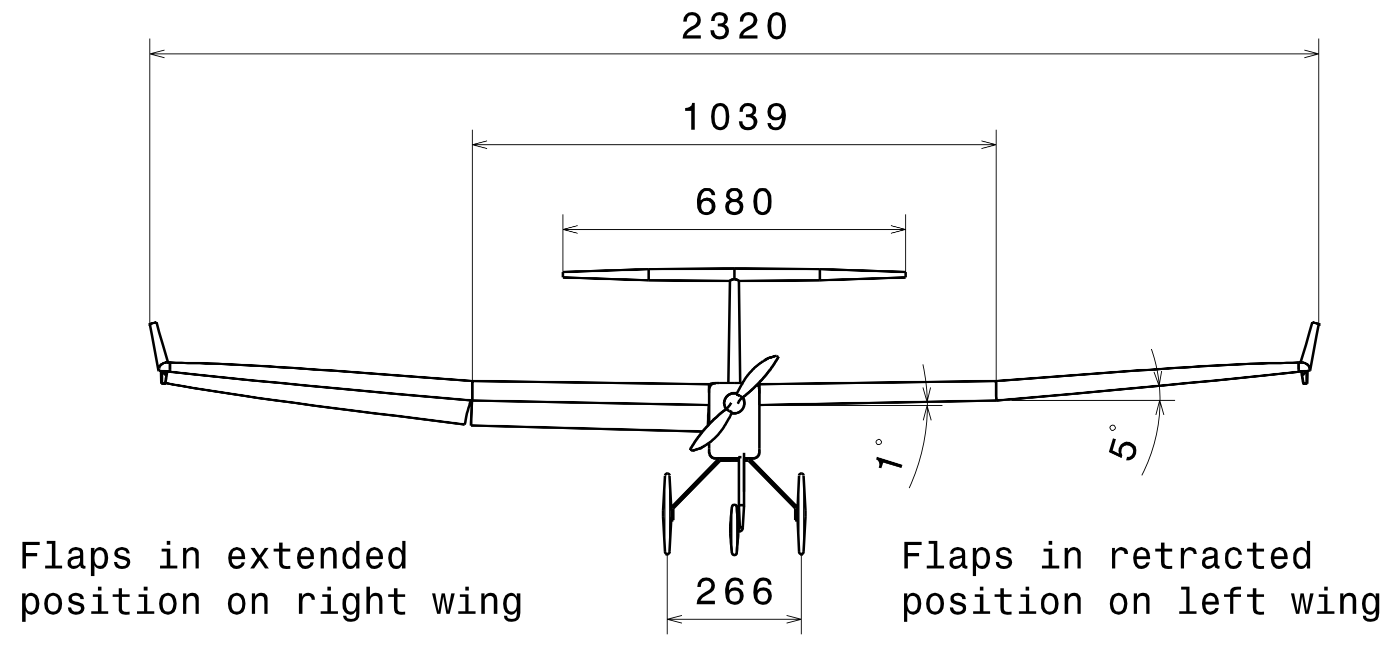


Front View

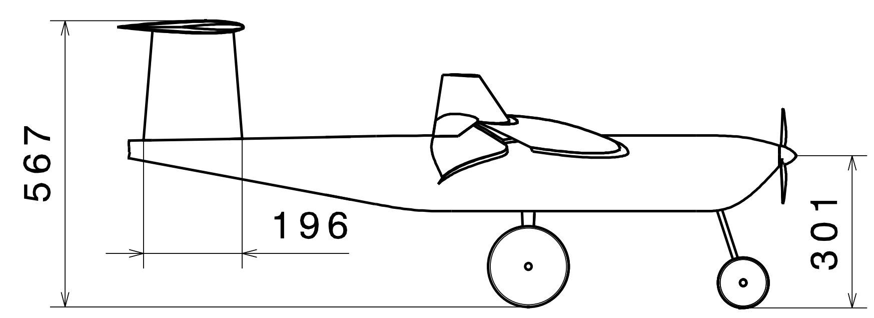


Side View

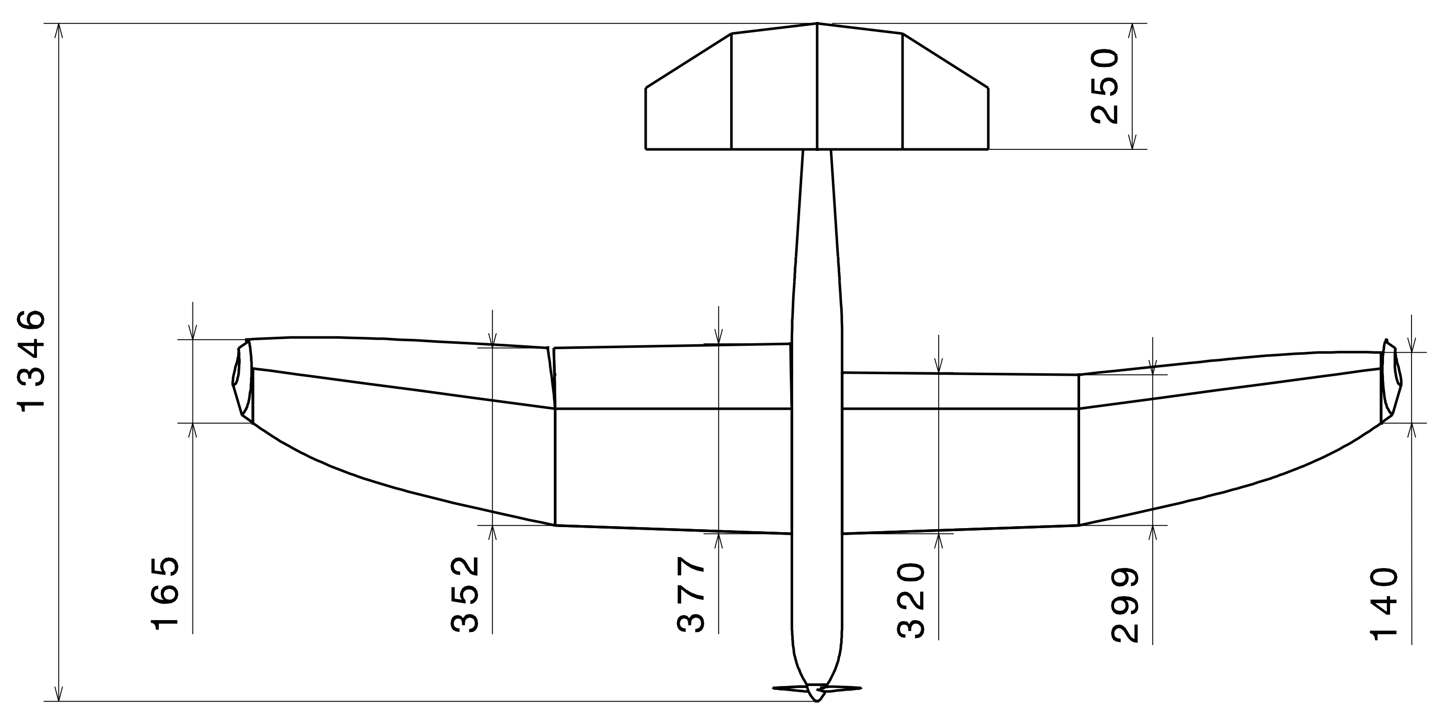


Top View

| Element | Area [m²] | Volume coefficient [-] |
|---|---|---|
| Wing | 0,61 | - |
| Horizontal tail | 0,145 | 0,583 |
| Vertical tail | 0,039 | 0,018 |
| Airfoil | ACC22_V19 | |

| | | |
|---|---|---|
| All lengths in [mm] | 3-View Drawing | Drawing 1/4 |
| Universität Stuttgart | | Team number 16 |
| | AkaModell Stuttgart | Scale 1:15 |

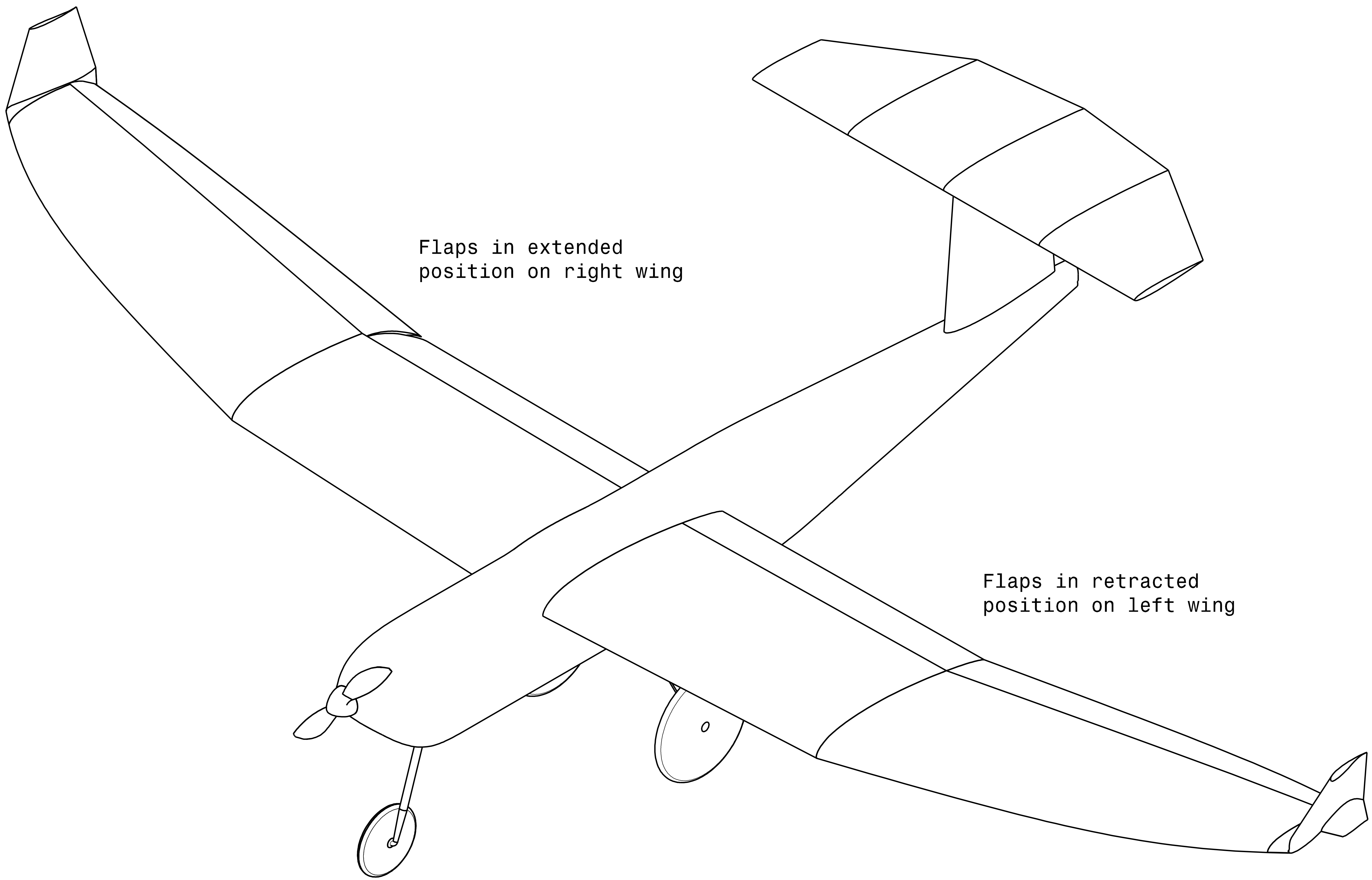


| | | |
|---|---|---|
| All lengths in [mm] | Isometric view | Drawing 2/4 |
| Universität Stuttgart | AkaModell Stuttgart | Team number 16 |
| | | Scale 1:5 |

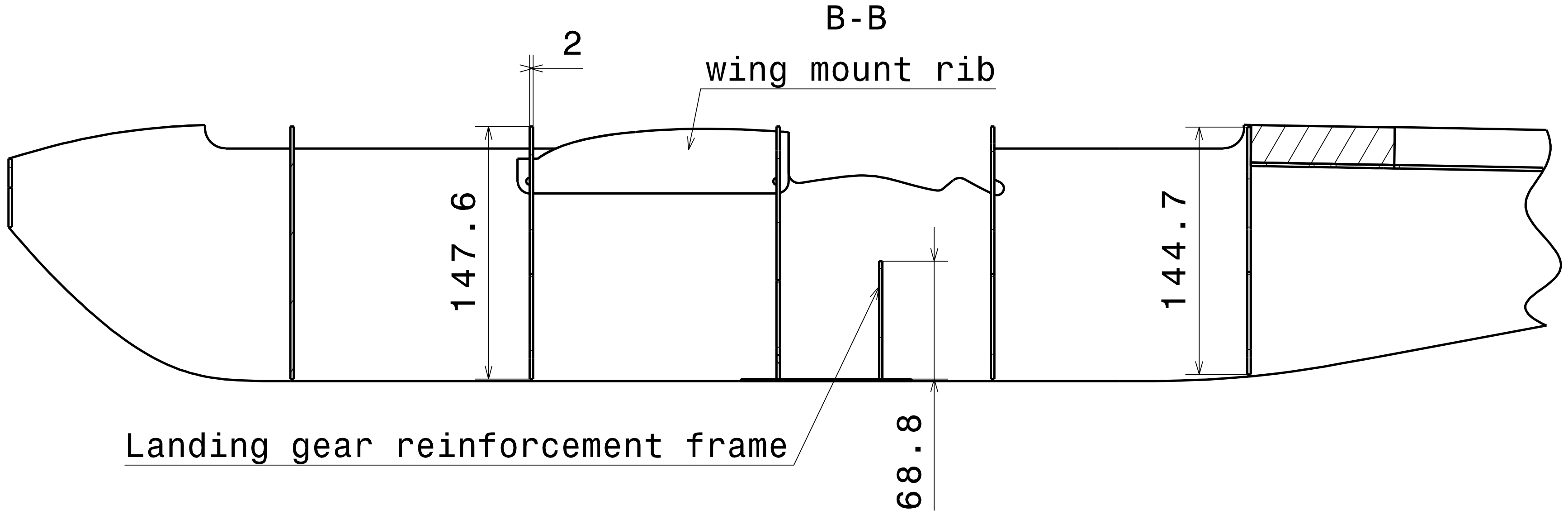


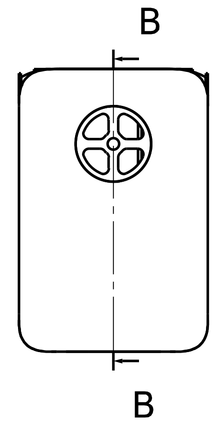


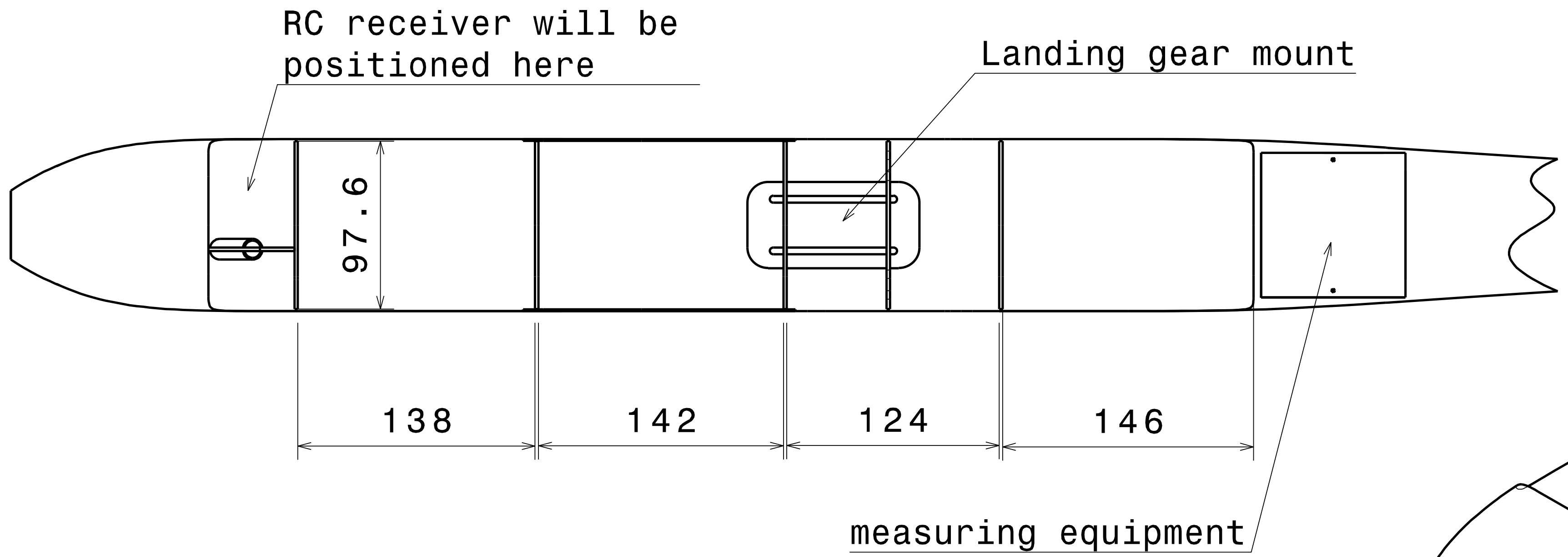


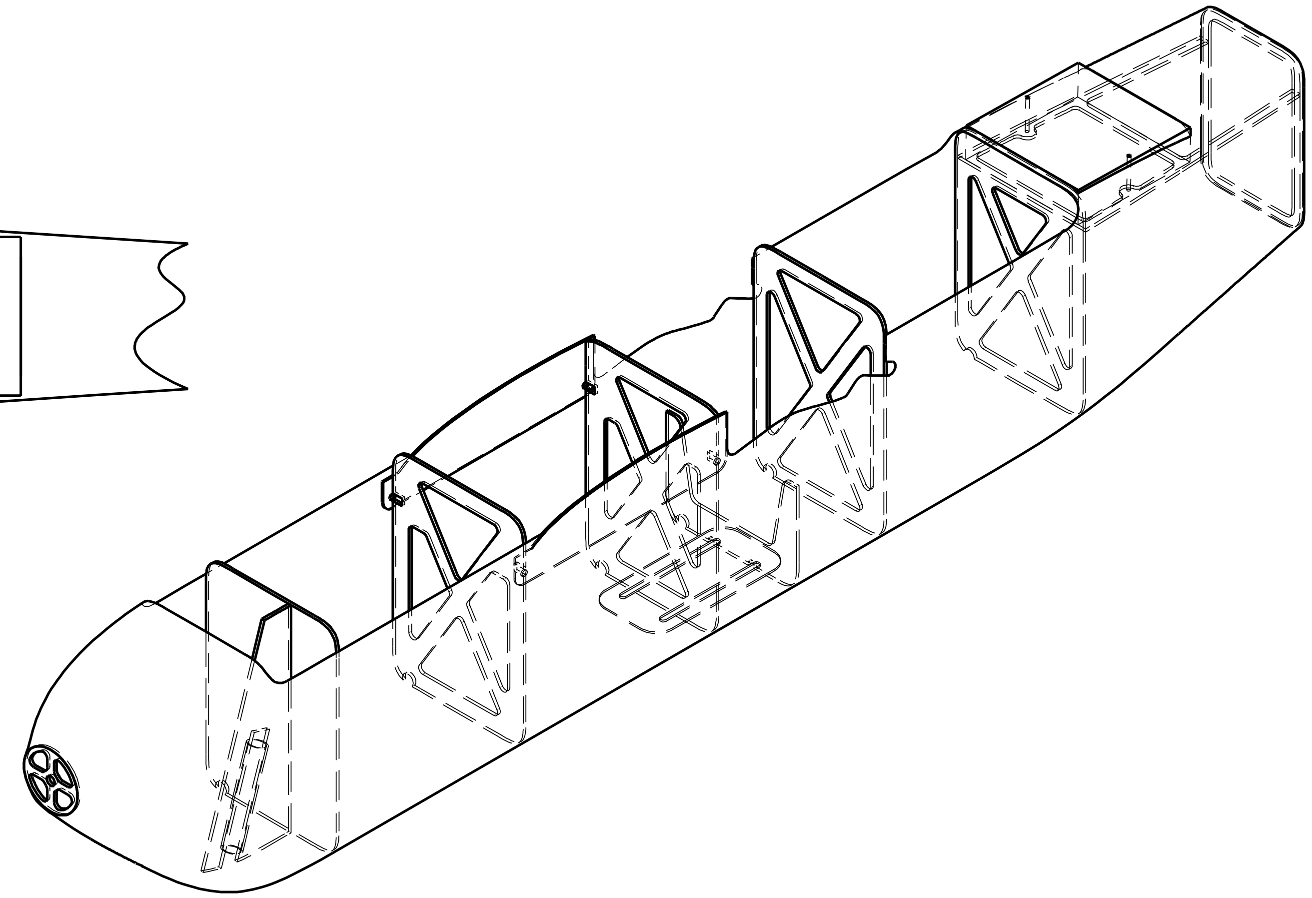

Cargo bags are positioned vertically between the frames in the fuselage pod. The exact position is dependend on the desired COG

| Maximum Cargo Volume | 7,7dm³ |
|---|---|

| All lengths in [mm] | Cargo Bay | Drawing 3/4 |
|---|---|---|
| Universität Stuttgart | | Team number 16 |
| | AkaModell Stuttgart | Scale 1:4 |

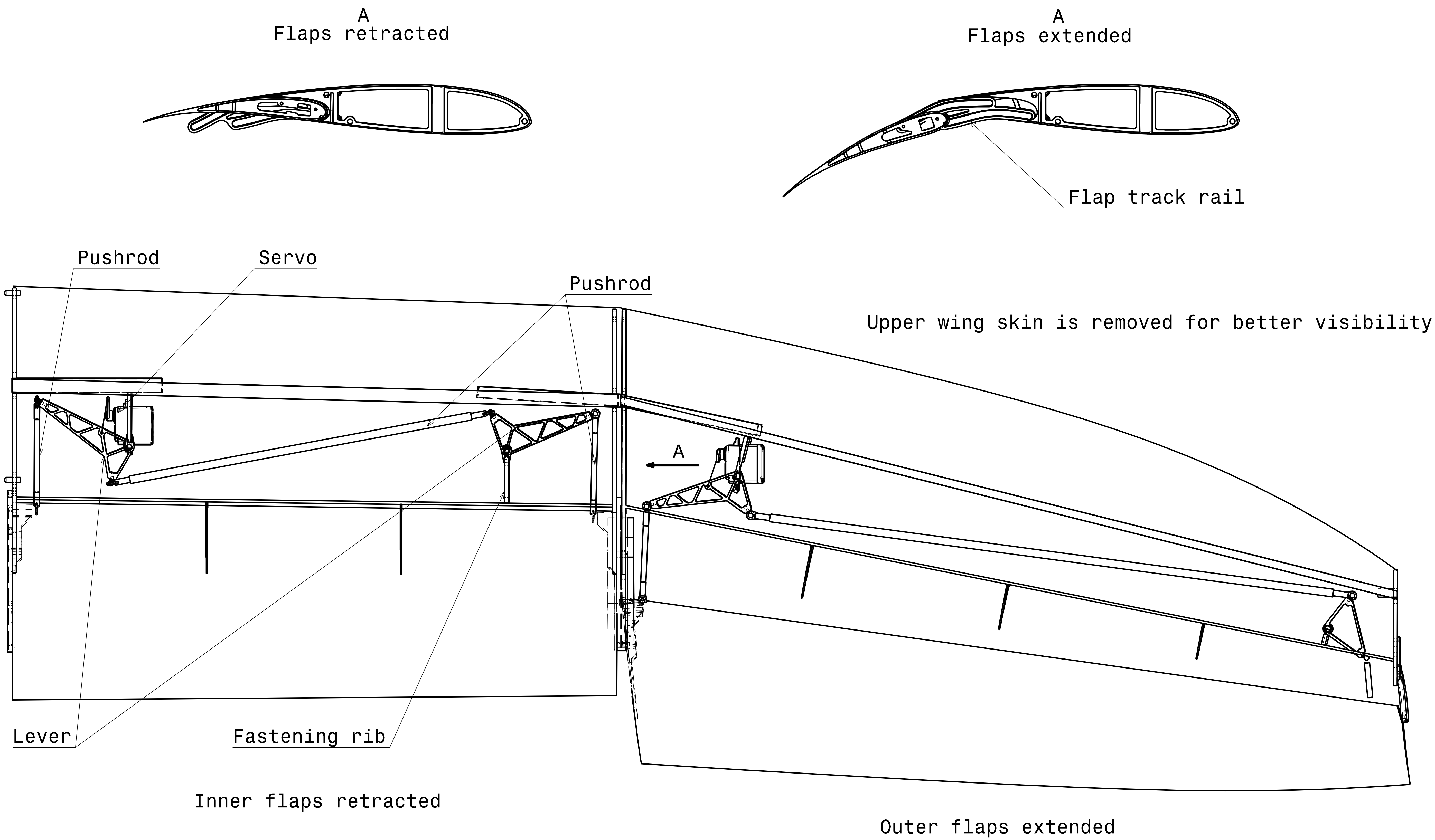


| | | |
|---|---|---|
| All lengths in [mm] | Slotted Flap Kinematic | Drawing 4/4 |
| Universität Stuttgart | | Team number 16 |
| | AkaModell Stuttgart | Scale 1:3 |